

58930-00-105
58926-00-105
58916-00-105

RECEIVED

DEC 06 1996 CONF-961040--17

OSTI ANL/MSD/CP--91227

Early Stages in the High Temperature Cyclic Oxidation of β -NiAl: An X-Ray Reflectivity Study

G. Muralidharan,¹ X.Z. Wu,^{1,2} Hoydoo You,¹ A.P. Paulikas,¹ and B.W. Veal¹

¹Materials Science Division, Argonne National Laboratory, Argonne, IL 60439

²Physics Department, Northern Illinois University, DeKalb, IL 60115

The submitted manuscript has been created by the University of Chicago as Operator of Argonne National Laboratory ("Argonne") under Contract No. W-31-109-ENG-38 with the U.S. Department of Energy. The U.S. Government retains for itself, and others acting on its behalf, a paid-up, nonexclusive, irrevocable worldwide license in said article to reproduce, prepare derivative works, distribute copies to the public, and perform publicly and display publicly, by or on behalf of the Government.

Proceedings of the 190th Meeting of the Electrochemical Society, San Antonio, TX, October 6-11, 1996

MASTER

DISCLAIMER

This report was prepared as an account of work sponsored by an agency of the United States Government. Neither the United States Government nor any agency thereof, nor any of their employees, makes any warranty, express or implied, or assumes any legal liability or responsibility for the accuracy, completeness, or usefulness of any information, apparatus, product, or process disclosed, or represents that its use would not infringe privately owned rights. Reference herein to any specific commercial product, process, or service by trade name, trademark, manufacturer, or otherwise does not necessarily constitute or imply its endorsement, recommendation, or favoring by the United States Government or any agency thereof. The views and opinions of authors expressed herein do not necessarily state or reflect those of the United States Government or any agency thereof.

This work supported by the U.S. Department of Energy, Basic Energy Sciences-Materials Science under Contract #W-31-109-ENG-38.

DISTRIBUTION OF THIS DOCUMENT IS UNLIMITED

29

DISCLAIMER

Portions of this document may be illegible in electronic image products. Images are produced from the best available original document.

EARLY STAGES IN THE HIGH TEMPERATURE CYCLIC OXIDATION OF β -NiAl: AN X-RAY REFLECTIVITY STUDY

G. Muralidharan[¶], X. Z. Wu^{¶§}, Hoydoo You[¶], A. P. Paulikas[¶] and B.W. Veal[¶]

[¶]Materials Science Division,
Argonne National Laboratory, Argonne, IL-60439.

[§]Physics Department, Northern Illinois University,
DeKalb, IL- 60115.

ABSTRACT

Early stages in the cyclic oxidation of β -NiAl at 500°C, 600°C, 700°C and 800°C were investigated using the technique of x-ray reflectivity. By fitting the data to a model function, oxide layer thickness, roughness of the oxide-vapor interface, and the roughness of the oxide-substrate interface were obtained as a function of oxidation time and temperature of oxidation. The time dependence of the oxide thickness was observed to be logarithmic at lower temperatures (500°C and 600°C) while a conventional $t^{0.5}$ kinetics was observed at the higher temperatures. Comparison of the roughness of the oxide-substrate interface with that of the oxide-vapor interface shows that for comparable oxide thicknesses and identical substrate conditions, the oxide-vapor interface was rougher than the oxide-substrate interface at all temperatures. This is consistent with the previously postulated growth mechanism (outward diffusion of cations) for oxide growth during the early stages of oxidation at these temperatures. Thus, x-ray reflectivity offers a convenient way of determining the oxide growth rates, and the roughness of the interfaces when the oxide layer is thin; this regime cannot be easily studied with the techniques that are currently used for oxidation studies.

INTRODUCTION

Metals and alloys in common technological applications are subject to external and internal oxidation. This is particularly true of high-temperature materials that are exposed to aggressive environments. Many technologically important alloys are protected by the formation of dense oxide scales that limit further oxidation of the underlying material. Al_2O_3 and Cr_2O_3 are two of the common oxides that form on high temperature alloys. Due to the technological importance of these oxides, the phenomenon of high temperature oxidation has been extensively studied in the past and is an active area of current research. (1,2). However, most studies concentrate on the growth of thick oxide scales (greater than 1 μ m in thickness); hence the techniques needed for the study of thicker oxide scales are better developed than those that have to be used for thin oxide scales. In recent years, it has been realized that the study of the early stages of oxidation is extremely important since in many cases, the oxides formed in the early stages dictate the evolution of the scale at the later stages of oxidation. Hence, more studies are being initiated to understand the early stages of oxidation.

One of the materials that holds promise for future high temperature use is β -NiAl (3). Although there are many studies that have focussed on the later stages of oxide growth, relatively few studies have looked at the very early stages of oxide scale evolution in this material. Doychak *et al.* (4) studied the transient oxidation of single crystal β -NiAl of different orientations using transmission electron microscopy and thermogravimetric measurements. They found that various forms of Al_2O_3 along with a spinel (NiAl_2O_4) could form depending on the temperature of oxidation, orientation of the substrate, and total oxidation time. No other oxide phases were identified in the samples oxidized at 800°C for various times up to 100 hours and at 1100°C for up to an hour of oxidation. Based on the morphology of the oxide that was formed on the surface, they argue that unlike the stable α - Al_2O_3 that grows by the inward diffusion of oxygen (or in some cases by a combination of the inward diffusion of oxygen and the outward diffusion of cations), metastable forms of Al_2O_3 grow predominantly by the outward diffusion of cations.

Understanding the growth mechanisms of oxides has been an area of considerable research interest (5-10). In addition to determining the rate of oxidation, the growth mechanism also influences the morphologies of the oxide-vapor and the oxide-substrate interfaces. Stresses that are developed in the oxide-substrate system during oxidation and the adherence of the scale to the substrate during oxidation under different environmental conditions are also affected by the growth mechanism of the oxide. Detailed studies of oxide growth mechanisms in β -NiAl at 900°C and 1000°C using inert markers, or by oxidation using a combination of ^{18}O and ^{16}O along with characterization using Rutherford back-scattering, have clearly shown that the cubic Al_2O_3 phases (θ , δ , γ) grow predominantly by the outward diffusion of Al (5-8). However, significant difficulties exist in the determination of the oxide growth mechanism since there are very few techniques that can probe the growth of oxides without interfering with the oxidation process. For example, deposition of inert markers has been known to lead to incorrect conclusions regarding the growth mechanism as a result of island formation (4-7). Difficulties also exist in determining the kinetics of oxide growth in the early stages of oxidation (primarily accomplished by *in-situ* thermogravimetric measurements), particularly at lower temperatures since the oxide layers are very thin and the rate of change of the thickness is small. This is probably one of the reasons for the lack of reliable kinetics data for the growth of transition aluminas in β -NiAl at temperatures below 900°C (5,6).

In this study, we present some of the results of our x-ray reflectivity study on the early stages of oxidation in β -NiAl in the temperature regime where oxide growth data are not available. Our results will demonstrate that this technique offers a convenient way of following the growth of the oxide without some of the difficulties mentioned above.

Principles of Specular X-ray Reflectivity

X-ray reflectivity has become a very popular technique for the study of various kinds of thin films ranging from metallic to organic films and for the study of surfaces(11). There have been a few x-ray reflectivity studies aimed at understanding the formation of oxide layers during electrochemical reactions (12), but very few efforts to examine the use of

reflectivity for studying thermally grown oxide scales. Specular X-ray reflectivity can probe the electron density profile normal to the surface; this density profile is clearly affected by the thickness of the oxide layer, the electron density of the oxide and the substrate, and the width of the oxide-air and the oxide-substrate interface. The experiment consists of measuring the specularly reflected intensity by placing the detector in the reflection plane with the angle of detection β being equal to the angle of incidence α . In this geometry, the direction of the momentum transfer $q = k_{\text{out}} - k_{\text{in}}$ is normal to the surface and its magnitude is given by:

$$q = q_z = \left(\frac{4\pi}{\lambda}\right) \sin \alpha, \quad [1]$$

where the x-ray wavelength $\lambda = 1.54 \text{ \AA}$ (Cu K_{α}) for our experiments. Thus the reflectivity $R(q_z)$, the intensity of specular reflection normalized by the incident intensity as a function of q_z , yields information about the electron density profile normal to the surface.

To obtain the parameters of interest, namely, film thickness, electron density profiles and interface widths, the variation in reflectivity as a function of q_z has to be modeled and fit to the measured one. For an ideally flat surface of electron density ρ_e , the reflectivity $R(q_z)$ is described by the Fresnel reflectivity $R_F(q_z)$:

$$R_F(q_z) = |r|^2 = \left| \frac{q_z - \sqrt{q_z^2 - q_c^2}}{q_z + \sqrt{q_z^2 - q_c^2}} \right|^2 \quad [2]$$

with

$$q_c = \left(\frac{4\pi}{\lambda}\right) \sin \alpha_c \quad [3]$$

and the critical angle

$$\alpha_c = \sqrt{\frac{r_e \lambda^2 \rho_e}{\pi}} \quad [4]$$

where r_e is the classical electron radius e^2/mc^2 , and ρ_e is the electron density of the material at the surface. $R_F(q_z)$ is unity for $q < q_c$, and decreases as $\left(\frac{q_c}{2q_z}\right)^4$ for $q \gg q_c$. Instead of the single electron density considered above, if the layer has a density profile varying in the z direction (but laterally homogeneous), the layer of finite thickness can be divided into infinitesimally thin layers with the electron density in each of the layers assumed to be a constant. At each interface between these thin layers, x-rays are either reflected or transmitted. By accounting for all of the waves transmitted and reflected at each interface, the reflectivity $R(q_z)$ can be calculated. For this physical model, $R(q_z)$ is approximately related to the electron density profile $\rho_e(z)$ through:

$$R(q_z) = R_F(q_z) \left| \frac{1}{\rho_\infty} \int_0^\infty \frac{\partial \rho(z)}{\partial z} \exp(iq_z z) dz \right|^2 \quad [5]$$

where ρ_∞ is the electron density deep inside the substrate. It is assumed that the substrate is homogeneous prior to oxidation and that, with oxidation, composition gradients will develop only near the surface of the substrate.

Expression [5] can be used to model reflectivity from a one-layer system, consisting of a uniform surface layer of thickness D with its electron density ρ different from the bulk ρ_∞ . (No composition gradients in the substrate are considered here). X-rays reflected from both interfaces of this surface layer interfere with each other and produce modulations in the reflectivity $R(q_z)$. This simple model has to be modified to include finite interface width σ . The diffuse interfaces are modeled as rough interfaces with the thickness modified by a roughness factor. If the roughness at each interface is modeled as Gaussian, the reflection coefficient R , eq. [5], becomes(12),

$$\begin{aligned} \frac{R(q_z)}{R_F(q_z)} = & \left(\frac{\rho}{\rho_\infty}\right)^2 \exp(-q_z^2 \sigma_1^2) + \left(\frac{\rho_\infty - \rho}{\rho_\infty}\right)^2 \exp(-q_z^2 \sigma_2^2) + \\ & 2 \frac{\rho(\rho_\infty - \rho)}{\rho_\infty^2} \exp(-q_z^2 (\frac{\sigma_1^2 + \sigma_2^2}{2})) \cos(q_z D) \end{aligned} \quad [6]$$

where σ_1 and σ_2 are roughnesses of the top and the buried interfaces respectively. The period of the modulation Δq_z is related to the layer thickness D as $\Delta q_z = 2\pi/D$, and the amplitude of the modulation depends on the difference between the electron densities in the bulk and in the surface layer. Equation [6] also shows that an increase in the roughness of either or both interfaces (increase in σ_1 or σ_2 or both) results in a reduction in the specular intensity and a damping of the modulation.

Modeling oxide growth

Even from the early stages of oxidation, the oxide layer is a distinct layer with electron density different from that of the matrix. Using x-ray reflectivity measurements, the oxide layer thickness, average electron density of the oxide and the matrix, and interfacial widths of the oxide-substrate interface and the oxide-gas interface can be probed. However, the above parameters cannot all be determined uniquely from reflectivity measurements. More than one combination of parameters might result in a satisfactory fit to the measured curve. Consequently, supplementary information must be available from independent experimental measurements in order to identify the correct combination of parameters that satisfy the physical model. For example, if a density ρ for the oxide results in a satisfactory fit for the reflectivity curve, a density $(\rho_{\infty} - \rho)$ will also result in a satisfactory fit for the same curve. However, since the oxide densities can be determined from independent measurements, the proper combination of parameters can be selected. Hence, for the present study, information obtained from previous studies on early stages of oxidation of β -NiAl along with atomic force microscopy measurements of the oxide surface have been used to complement the reflectivity measurements.

Our studies are limited to scales which consist primarily of cubic transition aluminas. Based upon previous studies (4-6), no phase transformation from the transition aluminas to the stable α -Al₂O₃ is expected for the exposure times and temperatures, and for scale thicknesses encountered in this study. Hence, the growth of these oxides can be conveniently simulated with a simple one-layer model. Figure 1 shows the electron density profile obtained for the system under consideration. The electron density for stoichiometric β -NiAl was calculated to be 1.7 Å⁻³ while the one for Al₂O₃ was estimated to be 1.1 Å⁻³. Since Gaussian roughness was assumed, the electron density variation at the interface was modeled as an error function. Although more elaborate models can be assumed for describing the interfacial roughness, it is believed that the assumption of Gaussian roughness is a satisfactory approximation for the experimental conditions used in the present series of measurements.

EXPERIMENTAL METHOD

β -NiAl with nominal composition 53 at.% Ni and 47 at.% Al was cast from electrolytically pure Ni and pure Al (99.99%) using an arc-melting furnace equipped with a water-cooled copper hearth. A single-crystal boule 38 mm. in diameter and 13 mm. thick was grown from this ingot by the vertical Bridgman growth technique in an ASTRO furnace. The boule was then oriented along a [110]-type direction and a cylindrical piece of thickness 5 mm. was cut from the center using electric discharge machining. This sample was used for further oxidation studies. Prior to each set of oxidation steps at a specific temperature, the sample was polished using standard metallographic procedures. Typically, grinding was done through 600 grit SiC paper followed by successive polishing using 5 μ m and 1 μ m Al₂O₃ grits. Final polishing was done with 0.05 μ m Al₂O₃. The polished sample was ultrasonically cleaned, and dried. The polishing procedure produced a surface

with a typical RMS roughness of 6 Å within the x-ray coherence length of approximately 0.5 μm.

Oxidation was carried out by placing the sample on a platinum foil which was inserted through a peep-hole into a box furnace maintained at the desired temperature. This facilitated rapid heating of the sample to a specified temperature and permitted quick removal of the sample after the oxidation treatment. Since the reflectivity measurements were made at room temperature, samples were thermally cycled between room temperature and the temperature of oxidation. Separate sets of thermally cycled oxidation experiments were carried out at 500°C, 600°C, 700°C and 800°C. Oxidation was carried out in air for predetermined lengths of time. X-ray reflectivity measurements were performed using a four-circle diffractometer and a rotating anode source equipped with a copper anode. Both specular intensities and the background were measured as a function of q_z . Using the oxide layer thickness, electron densities of the oxide and substrate and interfacial roughnesses as fit parameters in an iterative non-linear regression fitting routine, proper fits to the x-ray reflectivities were obtained.

RESULTS AND DISCUSSION

Figure 2 shows the reflectivity profiles obtained as a function of oxidation time at 500°C. Total oxidation time for each of these profiles is indicated in the figure. The first profile shown in the figure is from the as-polished surface. From the fitting process, it was determined that the RMS surface roughness of the sample was about 5 Å and that there was a native oxide layer with a thickness of about 12 Å. The thickness of the native layer in the as-polished condition prior to oxidation at 600°C, 700°C and 800°C ranged from approximately 10 Å to 30 Å. After characterizing the sample in the as-polished condition, the sample was oxidized at 500°C for a pre-determined length of time and then cooled down to room temperature for reflectivity measurements. Effect of the developing oxide layer on the reflectivity profile is seen clearly in the sequence of curves in figure 2. For example, the profile obtained after oxidizing for 30 minutes at 500°C reveals intensity modulations. Fitting the reflectivity profile using the one-layer model showed that the oxide layer is now about 60 Å thick, the RMS roughness of the oxide-vapor interface was about 10 Å, and the roughness of the buried interface was about 3.5 Å. With successive oxidation treatments, the oxide layer increased in thickness, and the roughness of both the oxide-substrate interface and the oxide-vapor interface increased.

Figure 3 shows the variation in scale thickness as a function of oxidation time at 500°C, 600°C, 700°C and 800°C. Note that the Wagner theory (1,2), which predicts that the thickness of the oxide layer should vary as $t^{0.5}$, is not applicable to the data obtained at 500°C and 600°C. These two sets of data are better characterized by a logarithmic time dependence (as indicated in the figure). It should be recalled that the Wagner theory assumes that space charge effects are negligible, the oxide is close to stoichiometry, and that the rate-controlling step is the volume diffusion of ions or electrons. Some of these assumptions are expected to be more appropriate for the later stages of oxide growth and hence it is not surprising that this theory is inapplicable for scale growth at these two temperatures. Although many theories have been proposed to explain the logarithmic

variation of the oxide thickness, very little is known about the mechanism of oxide growth that leads to this time-dependence (1, 2).

For oxidation at 700°C (and perhaps at higher temperatures), the scale growth appears to follow the Wagner theory. This is evidenced by the presence of linear behavior (above 600°C) in figure 4 where the square of the oxide thickness is plotted as a function of time. At 800°C, the oxide thickness increased rapidly and after just 15 minutes of oxidation, the magnitude of the modulations decayed to very low values due to the large roughnesses of the oxide-vapor and the oxide-substrate interfaces. This prevented further measurements at this temperature. As expected, the scale thickness after 15 minutes of oxidation at 800°C is much greater than the scale thickness after 15 minutes at 700°C.

There is very little experimental data in the literature pertaining to the kinetics of oxide growth in the temperature range examined in this study. Doychak *et al.* (4) measured the parabolic rate constants at 800°C for oxidation of samples of β -NiAl with a (011) orientation and obtained values of $8.06 \times 10^{-14} \text{ g}^2/\text{cm}^4\text{sec}$ and $6.73 \times 10^{-14} \text{ g}^2/\text{cm}^4\text{sec}$ for two different oxide textures. They reported rate constants of $6.42 \times 10^{-14} \text{ g}^2/\text{cm}^4\text{sec}$ and $8.45 \times 10^{-14} \text{ g}^2/\text{cm}^4\text{sec}$ for polycrystalline β -NiAl with the different values being obtained for different oxide textures. They comment that the data could be inaccurate due to the difficulties in performing the measurements. In the present series of experiments, due to the relatively large roughnesses ($>35 \text{ \AA}$) of the interfaces, the progress of oxidation could not be followed beyond 15 minutes at 800°C. However, an instantaneous growth rate of $3160.0 \text{ \AA}^2/\text{min}$ ($52.7 \text{ \AA}^2/\text{sec}$) was obtained from the two data points that were available for this temperature (figure 4). Assuming that the oxide consists primarily of γ - Al_2O_3 with a density of 4.12 gm./cm^3 , a parabolic rate constant of $8.95 \times 10^{-14} \text{ g}^2/\text{cm}^4\text{sec}$ was calculated for oxide growth at 800°C. This value is larger than those reported previously by Doychak *et al.* Although errors in the calculations of rate constant could have resulted in this difference, there is another factor that should be considered in this comparison. The single crystal samples used in the present study were mechanically polished before the oxidation treatment while Doychak *et al.* electropolished their samples before oxidation. Recent studies on mechanically polished samples similar to those used in the present study failed to show the presence of ion-channeling (13) which indicates that prior to oxidation, there is a severely deformed layer extending at least a few hundred \AA below the polished surface. Since the temperatures used in the oxidation study were relatively low, it is possible that the presence of this damaged layer resulted in accelerated growth of the oxide. The presence of a deformed layer might also explain the dependence of oxidation rates on the degree of surface polish that is often reported in the literature (14). Further work is underway to explore this possibility.

Figure 5 shows the RMS roughness of the oxide-vapor interface (outer surface) and the oxide-substrate interface (buried interface) as a function of scale thickness resulting from oxidation at 500°C. Note that the roughness of the outer surface is greater than that of the buried interface. Analysis of the roughness data obtained during oxidation at 600°C, 700°C and 800°C also showed that the outer surface was always rougher than the buried interface for the experimental conditions used in this study. Recall that for the time and temperature combinations used in this study, the oxide is expected to grow by the outward diffusion of cations with the fresh oxide forming at the oxide-vapor interface (4-10). It is

likely that the larger roughness values at the oxide-vapor interface are a consequence of oxide growth occurring predominantly at the oxide-vapor interface. Thus, x-ray reflectivity measurements might provide direct information on the oxide growth mechanism.

Oxidation behavior was modified when the Al concentration in the near-surface region of the sample was changed by prior oxidation. Since Al is selectively removed from the matrix during oxidation, the near-surface region in an oxidized β -NiAl sample will have an Al content that is lower than the nominal Al content of the alloy. At 600°C, β -NiAl exists over the composition range 45.0 at.% Ni (55.0 at.% Al) to about 60.0 at.% Ni (40.0 at.% Al) (15). Since the composition of β -NiAl used in this study was 53.0 at.% Ni (47.0 at.% Al), significant changes in the composition of the sample near the surface can result from oxidation, with the near-surface region still being single-phase β -NiAl. For example, Bobeth *et al.* (16) found that the Al content in the near surface region in β -NiAl samples with a nominal composition of 50.5 at.% Al dropped to 46.0 at.% after 200 hours at 950°C but that it recovered to 48.0 at.% Al with further oxidation (500 hours).

The effect of Al depletion on the kinetics of oxide growth at 600°C on the β -NiAl sample used in this study is demonstrated in figure 6. This figure compares the growth of oxide on the same sample but with different initial conditions - in one case (open circles), the sample did not have a composition gradient resulting from a near-surface diffusion zone; in the second case (solid circles), a region with a composition gradient was introduced by oxidizing the sample for 57 hours at 500°C and subsequently removing the scale by mechanical polishing without removing much of the diffusion zone beneath the oxide. Note that for comparable oxidation times at 600°C, the scale is thinner on the sample with the near-surface Al depletion zone (figure 6(a)). The time dependence of scale thickness during oxidation is also different for the two sample conditions. The sample without the pre-existing composition gradient exhibits logarithmic growth kinetics while the sample with a near-surface Al depletion zone shows the more conventional $t^{0.5}$ kinetics. A change from logarithmic to parabolic kinetics during isothermal oxidation has been observed in other experimental studies(1). The change in growth kinetics in the present study indicates that oxide growth on the sample with the pre-existing Al gradient is diffusion limited while oxide growth on the sample without the Al depletion zone shows more complex growth mechanism. Also, these results suggest that with the development of a region depleted in the oxide-forming element, oxidation becomes diffusion limited and scale growth tends toward $t^{0.5}$ kinetics.

Significant differences in the evolution of roughness at the oxide-substrate and the oxide-vapor interfaces were also observed for these two sample conditions (figure 6 (b)). Recall that for the initially homogeneous sample, the outer surface was rougher than the buried interface for all oxidation conditions examined (figure 5). However, for the scale formed on the sample with a pre-existing Al depletion zone, the buried interface was rougher than the outer surface for all stages of oxidation examined at 600°C.

The observations outlined here clearly indicate that the early stage of oxidation is influenced by the development of a region depleted in the oxide-forming element. The absence of logarithmic growth kinetics in samples with a pre-existing Al gradient suggests that the transition from logarithmic to parabolic growth kinetics is related to the

development of this diffusion zone. The dramatic change in the relative roughnesses of the outer surface and the buried interface accompanied by a change in the kinetics of oxide growth suggests that the oxide growth mechanism is affected by the presence of this depletion zone.

CONCLUSIONS

Specular X-ray reflectivity was used to study the early stages of oxidation of a (011) - oriented single crystal sample of β -NiAl at various temperatures in the range 500°C to 800°C. At these temperatures, the oxide scale is expected to consist primarily of cubic transition aluminas. From the reflectivity measurements, the thickness of the oxide scale, RMS roughnesses of the oxide-vapor interface (outer surface) and oxide-substrate interface (buried interface) were obtained as a function of the temperature of oxidation and oxidation time. For oxidation at 600°C and lower, the oxide layer showed logarithmic growth kinetics. Oxidation at 700°C resulted in a parabolic growth behavior in agreement with the Wagner theory of oxidation, thus suggesting a diffusion limited growth mechanism. It was also observed that the RMS roughness of both the oxide-substrate and the oxide-vapor interfaces increased as a function of oxidation time at all temperatures. However, the relative values of the two roughnesses was found to be dependent on the initial sample condition. When the sample was initially homogeneous with respect to the Al content, the outer surface was found to have an RMS roughness larger than that of the buried interface for the conditions used in this study. When an Al composition gradient was introduced by prior oxidation, the buried interface had a larger RMS roughness than the outer surface. Thus, reflectivity measurements show that the establishment of a depletion zone plays an important role in the early stage oxidation behavior.

ACKNOWLEDGMENTS

The submitted manuscript has been created by the University of Chicago as Operator of Argonne National Laboratory ("Argonne") under contract No. W- 31-109-ENG-38 with the U.S. Department of Energy. The U. S. Government retains for itself, and others acting on its behalf, a paid-up, nonexclusive, irrevocable worldwide license in said article to reproduce, prepare derivative works, distribute copies to the public, and perform publicly and display publicly, by or on behalf of the Government. X.Z.W. would also like to thank the State of Illinois for support under HECA.

REFERENCES

1. Per Kofstad, High-Temperature Corrosion, Elsevier Applied Science, London, 1988.
2. N. Birks and G. H. Meier, Introduction to High Temperature Oxidation of Metals, Edward Arnold, 1983.
3. D. B. Miracle and R. Darolia, Intermetallic Compounds: Vol. 2: Practice, Eds. J. H. Westbrook and R. L. Fleischer, John Wiley, NY, 53 (1994).
4. J. Doychak, J. L. Smialek and T. E. Mitchell, Metall. Trans., 20 A, 499 (1989).

5. J. Doychak, *Intermetallic Compounds: Vol. 1, Principles*, Eds. J. H. Westbrook and R. L. Fleischer, John Wiley, NY, 977 (1994).
6. R. Prescott and M. J. Graham, *Oxidation of Metals*, **38**, Nos. 3/4, 233 (1992).
7. E. W. A. Young, J. C. Rivière and L. S. Welch, *Appl. Surf. Sci.*, **31**, 370 (1988).
8. E. W. A. Young, J. C. Riviere and L. S. Welch, *Appl. Surf. Sci.*, **28**, 71 (1987).
9. G. C. Rybicki and J. L. Smialek, *Oxid. Metals*, **31**, Nos. 3/4, 275 (1989).
10. B. A. Pint, J. R. Martin and L. W. Hobbs, *Solid State Ionics*, **78**, 99 (1995).
11. G. S. Knapp, M. A. Beno and H. You, *Annu. Rev. Mater. Sci.*, **26**, 693 (1996) and references therein.
12. H. You, C. A. Melendres, Z. Nagy, V. A. Maroni, W. Yun and R. M. Yonco, *Phy. Rev. B*, **45**, No. 19, 11288 (1992).
13. G. Muralidharan, X. Z. Wu, B. W. Veal, A. P. Paulikas, P. M. Baldo and L. E. Rehn, unpublished work, Argonne National Laboratory, 1995.
14. R. Hutchings and M. H. Loretto, *Metal Science*, Nov., 503 (1978).
15. P. Nash, M. F. Singleton and J. L. Murray, *Phase Diagrams of Binary Nickel Alloys*, ASM, Materials Park, OH, 3 (1991).
16. M. Bobeth, E. Bischoff, E. Schumann, M. Rockstroh and M. Rühle, *Corrosion Science*, **37**, No. 4, 657 (1995).

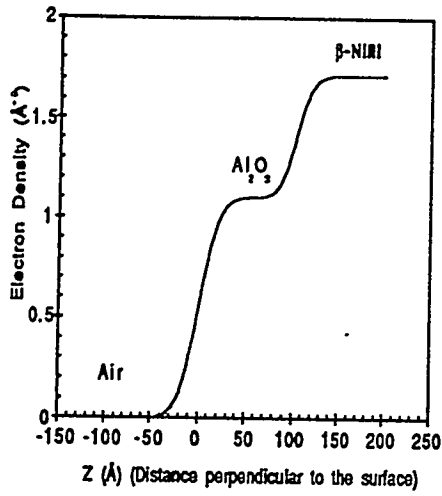


Figure 1. Electron density profile for a 100 Å thick oxide layer of Al_2O_3 on a $\beta\text{-NiAl}$ substrate.

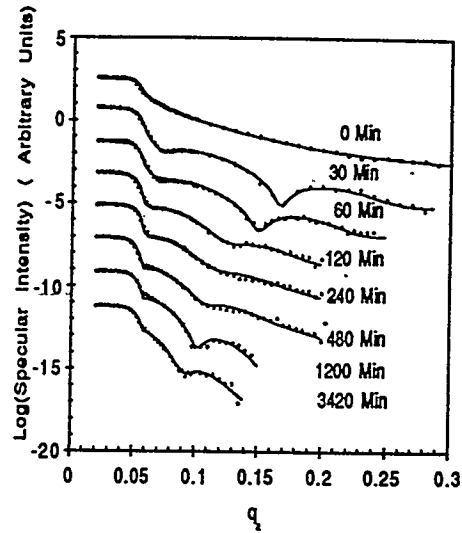


Figure 2. Reflectivity as a function of oxidation time at 500 °C

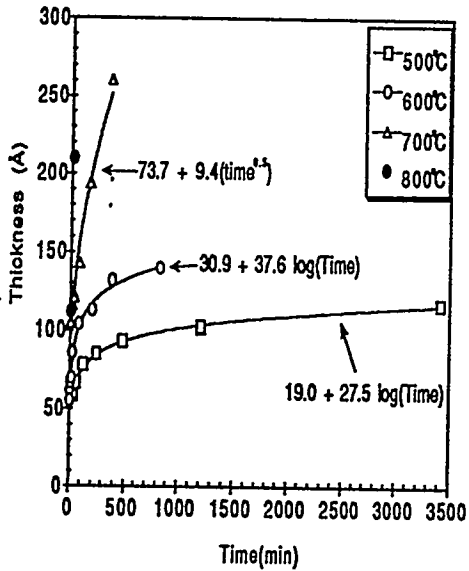


Figure 3 Variation in scale thickness as a function of time at different oxidation temperatures.

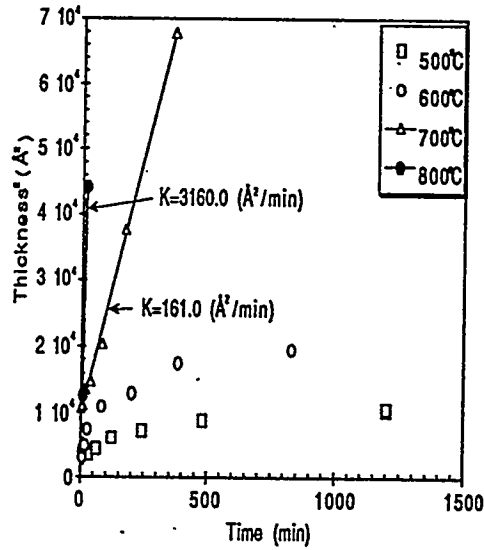


Figure 4. Variation in (thickness of oxide)² as a function of time.

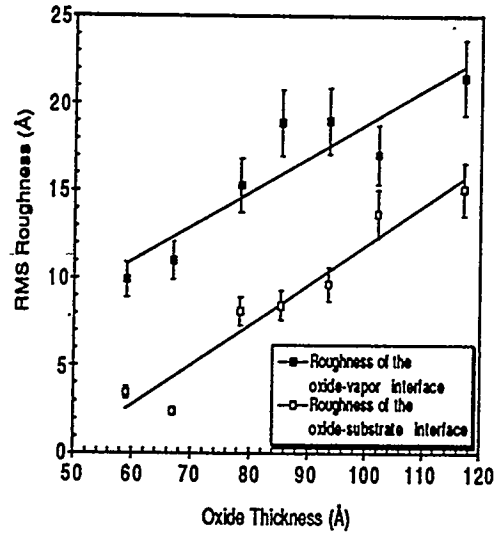
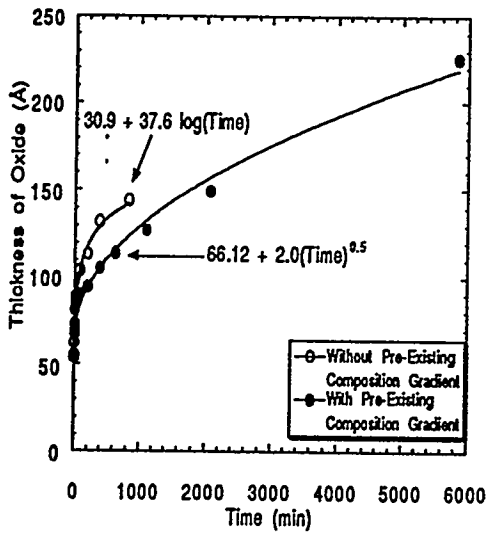
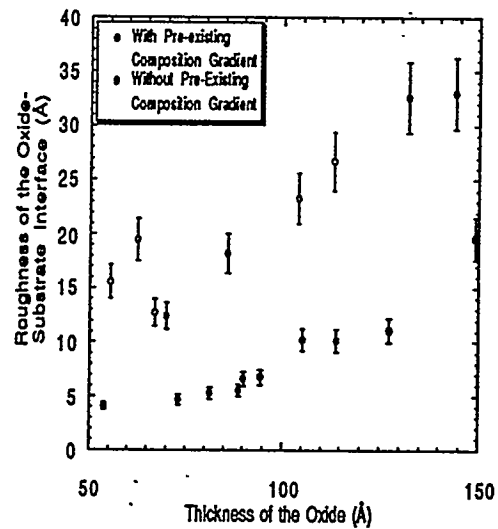


Figure 5. Variation in the RMS roughness of the oxide-vapor interface and the oxide substrate interface as a function of oxide thickness at 500°C obtained by fitting the data shown in Figure 2.



(a)



(b)

Figure 6. Effect of pre-existing near-surface aluminum depletion zone on (a) scale thickness as a function of oxidation time, and (b) roughness of the substrate-oxide interface (buried interface) as a function of oxidation time.